J. Fluid Mech. (1969), *vol.* 37, *part* 2, *pp.* 325–335
Printed in Great Britain

Experiments on shock stand-off distance in non-equilibrium flow

By PETER P. WEGENER AND GEORGE BUZYNA

Department of Engineering and Applied Science, Yale University,
New Haven, Connecticut

(Received 25 June 1968)

An experimental investigation of the non-equilibrium behaviour of the shock stand-off distance ahead of spheres at low supersonic Mach number is reported. An intermittent wind tunnel operating with a reacting gas mixture with one non-equilibrium mode is described. A non-equilibrium parameter after Damköhler is determined for the flow and the experiments cover a range of this variable from near-frozen to near-equilibrium states. The shock stand-off distance is measured and found to vary as expected between these two bounds with a low value at equilibrium. With all other variables governing shock stand-off distance held constant, such measurements can also be used to determine the relaxation time of the non-equilibrium mode.

1. Introduction

The shock stand-off distance Δ, in front of a sphere of radius R, is largely a function of the density ratio across the shock wave as measured on the stagnation streamline (e.g. Hayes & Probstein 1966, p. 284). Consequently, the dimensionless ratio Δ/R is sensitive to Mach number at low supersonic speeds, as seen in figure 1, and it approaches a constant value for strong shocks in hypersonic flow of thermally and calorically perfect gases. However, if processes such as vibrational excitation, dissociation, chemical reactions and ionization occur in the stagnation region, the density ratio between the free stream and the shock layer will be affected. Thus, other conditions remaining unchanged, a variation of the shock stand-off distance must be expected. The extent of this change owing to the vibrational excitation, the degree of dissociation, and the like in the flow field will be governed by a non-equilibrium parameter such as that proposed by Damköhler (1936) in his dimensional analysis of steady-state chemical flow reactors. Indeed, conversely, the stand-off distance may be regarded as a measure of the state of the gas in the region between shock and body as originally proposed by Schwartz & Eckerman (1956).

Much theoretical work on supersonic and hypersonic perfect gas flows about blunt bodies has been done in recent years. These studies were motivated by the practical importance of such flows, as well as by the inherent fundamental interest in mixed flow fields (e.g. Hayes & Probstein 1966). The additional complications

introduced by including real gas and non-equilibrium effects have, however, been tackled less frequently. Included in such theoretical studies relevant to our work we find the papers by Freeman (1958), Lick (1960), Hall, Eschenroeder & Marrone (1962), Lun'kin & Popov (1966) and Conti (1966).† Relatively few experimental results appear to be available on non-equilibrium stand-off distance of shock waves and those described in the literature were usually obtained in firing ranges. The first experiments of this type utilizing the vibra-

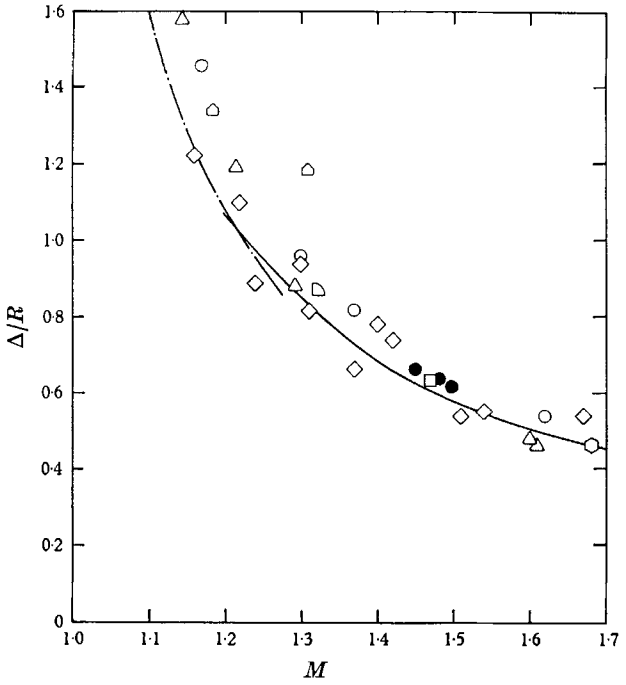

FIGURE 1. Dimensionless shock stand-off distance in front of spheres as a function of Mach number in a perfect gas with $\gamma = \frac{7}{5}$. Theoretical results: —·—, Moeckel (1949); ———, Van Dyke & Gordon (1959). Experimental results: ○, Heberle, Wood & Gooderum (1959); □, Kendall (1959); △, Charters & Thomas (Nagamatsu 1949); ◇, Puckett & Schamberg (Nagamatsu 1949); ⬠, Sugimoto (Van Dyke 1958); ⬡, Ladenburg *et al.* (Van Dyke 1958); ⌂, Jenkins, Jenkins & Johnson (1966); ●, present work.

tional excitation of chlorine gas as the non-equilibrium mode were presented by Schwartz & Eckerman (1956). In addition, Eckerman (1961) studied oxygen dissociation, Lobb (1963) worked with a number of non-equilibrium processes in air at high Mach numbers, and Zienkiewicz & Malloch (1968) provide results on vibrational relaxation of carbon dioxide. The experimental work to date shows the marked effect of real gas behaviour on stand-off distance clearly. However, in experiments with dissociation reactions, it seems that a number of physico-chemical processes or flow parameters were varied simultaneously. Such effects include Mach number changes and variation of static pressure or reactant pressure. It therefore appeared desirable to study experimentally the stand-off

† For additional papers we refer to the excellent summary by Hall & Treanor (1968).

distance of shock waves in front of spheres in terms of a single non-equilibrium parameter.

The dissociation reaction of nitrogen tetroxide carried in inert nitrogen, as given by

$$N_2 + N_2O_4 \rightleftharpoons N_2 + 2NO_2, \tag{1}$$

was chosen as a model gas mixture to study the non-equilibrium flow. The equilibrium properties and the rate constants of the system of equation (1) are known, and several other non-equilibrium flow problems were previously explored with this mixture in nozzles and a firing range, as referred to in Wegener, Chu & Klikoff (1965). A short-duration, intermittent wind tunnel, in part patterned after a device first proposed by Ludwieg (1955, 1957), was built for the experiments to be discussed here.

2. A non-equilibrium parameter

Chemists have long employed the intuitive concept of the product of reaction velocity and residence time to characterize chemical flow reactors. Förster & Geib (1934) first proposed a dimensionless parameter relating flow speed, diffusion rate, and the rate of a first-order reaction. The complete analysis of the relevant fluid-mechanical, molecular and chemical properties entering such complex systems is due to Damköhler (1936), whose first dimensionless parameter gives the ratio of a characteristic chemical time to that of a characteristic flow time. In analogy we shall use an inverse expression

$$D \equiv \tau_{\text{flow}}/\tau_{\text{chem}}, \tag{2}$$

in conformity with Freeman (1958). In general, we expect thermodynamic equilibrium in a flow field with $D = \infty$. Conversely, with $D = 0$ we have frozen flow, i.e. a flow in which the chemical change may be neglected. Between the two limits about the value $D \simeq 1$, we anticipate flow conditions that are governed by non-equilibrium effects.

Equation (2) may be applied to inviscid blunt-body flows at supersonic speed with a single reaction. In flows with given free-stream conditions we anticipate an upper or lower bound of Δ/R for $D = 0$ and $D = \infty$ respectively. The pressure in the shock region is found to be relatively unaffected by the reaction (Lick 1960, figure 7; Conti 1966, figure 3). On the other hand, the temperature in the equilibrium shock-layer is lower than that for frozen flow because the chemical (or other) excitation processes act as heat sinks. Consequently, the shock-layer density with reactions is greater than that for frozen flow, and the shock wave is closer to the body.

Next we express the non-equilibrium parameter, D, given by (2) for flow over a sphere, with the reacting gas mixture represented by (1). The characteristic flow time, τ_{flow}, may be defined by assuming a linear decrease of the flow velocity behind the normal shock, u_s, to zero speed at the stagnation point along the length Δ. This assumption gives a good approximation for perfect gas flow (Kendall 1959), and reacting flows are not expected to behave significantly differently (Lick 1960). We thus have:

$$\tau_{\text{flow}} \equiv \tau_\Delta \equiv \Delta/\tfrac{1}{2}u_s. \tag{3}$$

The reaction of (1) remains frozen across the normal shock so that u_s may be found directly from the Rankine–Hugoniot equations and the known state of the free stream.

A definition of a chemical relaxation time is less straightforward for our system. However, the differential equation of the reaction mechanism for (1) is known and its rate constants have been measured previously (Carrington & Davidson 1953; Wegener 1958). We can therefore express the rate law for (1) by

$$d\alpha/dt = L(p, \rho, \alpha), \tag{4}$$

where α is the degree of dissociation of the reactants, defined by

$$\alpha \equiv \omega_{NO_2}/(\omega_{NO_2} + \omega_{N_2O_4}),$$

with ω_i as the mass fraction of the ith species. Equation (4) may be integrated to give the variation of α with time in the non-equilibrium region behind the shock wave. Following Freeman (1958), a relaxation time, τ_r, may conveniently be defined by

$$\tau_r = t(0{\cdot}95\alpha_e) - t(\alpha_s), \tag{5}$$

giving a time in which α changes from the frozen value behind the shock, α_s, to a value of α that corresponds to 95 % of the new equilibrium value α_e. The equilibrium value α_e is obtained from a solution of the Rankine–Hugoniot equations for thermodynamic equilibrium. A typical value of τ_r for the experiments to be discussed later is 10 μs.

In addition to the relaxation time given by (5), an analytical expression for the chemical relaxation time may be defined by use of the well-known equations for the propagation of small disturbances in a relaxing flow, linearized about the state of equilibrium. Such a relaxation time of the linear theory, τ_ϕ, was derived previously, e.g. equation (6) of Wegener *et al.* (1965), for the system of (1) in conjunction with the linear form of (4). At the conditions behind the shock wave we find from the previous work:

$$\tau_\phi = -\frac{1}{\partial L/\partial\alpha}\frac{\partial h/\partial\rho}{\partial h/\partial\rho + (\partial h/\partial\alpha)(\partial\bar{\alpha}_e/\partial\rho)}, \tag{6}$$

with the enthalpy and density of the flow given by h and ρ respectively. The value $\bar{\alpha}_e$ refers to the local equilibrium degree of dissociation for conditions behind the shock wave. For a given experimental environment, (6) gives a value of the relaxation time that is about one-fifth of that found from (5).

With these definitions established, we may now define the Damköhler, or non-equilibrium parameter, from (2), (3), (5) and (6), in two ways:

$$D_r \equiv \tau_\Delta/\tau_r, \tag{7}$$

or

$$D_\phi \equiv \tau_\Delta/\tau_\phi. \tag{8}$$

Typical experimental values to be shown later apply to $0{\cdot}1 < D_r < 5$, and $0{\cdot}5 < D_\phi < 25$ for the two definitions of chemical relaxation time. The relaxation time in (8) is often simpler to compute and therefore this definition of D may be preferable. The numerical results based on the linear theory will also characterize the time scale of the rate of approach to equilibrium in a situation when only the non-linear rate equation (4) is valid (Zeldovich & Raiser 1966, p. 351). The

differences of the numerical values of D_r and D_ϕ arise in part from the arbitrary definition of τ_r in (5). Any decrease in the fraction of the degree of dissociation of α_e in the upper integration limit of (5) will increase the value of D_r in (7) to bring D_r closer to D_ϕ. For these reasons no physical significance ought to be attached to a particular choice of a chemical relaxation time as long as different experiments are compared on a consistent basis.

3. Experiments

An intermittent supersonic wind tunnel shown schematically in figure 2 was built for the experiments. This facility represents a modification of a device proposed by Ludwieg (1957). In our arrangement a cellophane diaphragm similar

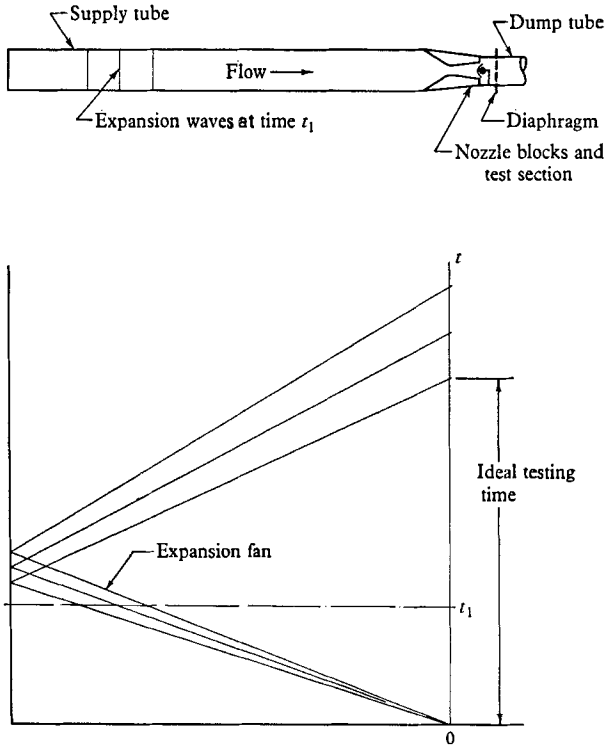

FIGURE 2. Intermittent wind tunnel. Supply tube, 5·3 in. inside diameter and 12 ft. in length; dump tube, 3·8 in. inside diameter and 14 ft. in length; two-dimensional nozzle with 2 in. × 2 in. throat; ideal testing time 20 ms.

to that used in shock tubes is located at the nozzle end and a dump tube is connected to the test section. The pressure or supply tube with the diaphragm in place is filled at room temperature with the carefully dried and well-mixed reacting gas mixture of (1), at about one atmosphere total pressure, and at a known reacting gas mass-fraction $\omega_R = \omega_{NO_2} + \omega_{N_2O_4}$. The reaction of (1) is rapid so that no handling operations disturb the known state of thermodynamic equilibrium. The dump tube is evacuated to a lower pressure ($< 0{\cdot}1$ atm), and external rupture of the diaphragm initiates the flow process. The ensuing tunnel

operation is also shown in figure 2 for the idealized situation of inviscid flow and instantaneous diaphragm removal. Left-facing expansion waves travel into the supply tube and accelerate the gas mixture toward the nozzle. After choking the nozzle throat at conditions determined by the ratio of the cross-sectional areas of the throat and the supply tube, the expansion ratio of the expansion fan becomes fixed, and steady flow through the nozzle begins. For inviscid flow this steady state of constant nozzle supply conditions behind the expansion fan, p_0, T_0 and ω_R, persists until the expansion waves reach the nozzle after reflexion at the supply tube end. Therefore, the useful testing time is linearly dependent on the length of the pressure tube. The nozzle consists of a converging–diverging pair of two-dimensional nozzle blocks. The nozzle is preceded by a transition section changing the flow from a circular to a rectangular cross-section. Plane walls are faired into a cylindrical throat-section ending with an exit cross-section of about 2×2 in. at a Mach number of about 1·5 for dry air. Sphere models mounted on a sting support can be moved axially to permit a slight Mach number variation. The models used were stainless steel ball-bearings of $\frac{1}{32}$, $\frac{1}{16}$, $\frac{1}{8}$, $\frac{1}{4}$, $\frac{1}{2}$ and $\frac{5}{8}$ in. diameter. After the initial shock system has passed around the model and other unsteady effects of about 5 ms duration have ceased, the flow becomes steady for about 15 ms.

Static and supply-pressure measurements with pressure transducers and high-speed movies of the flow about the spheres showed that the viscous effects in the supply tube could be disregarded within the measuring accuracy of about $\frac{1}{2}\%$ in pressure. This is in agreement with calculations based on Becker's (1958) analysis of this particular problem. The test-section Reynolds number for the experiments was of the order of 10^5/cm. The corresponding boundary-layer displacement thickness on the spheres (Schlichting 1960, p. 81) did not exceed 1% of the shock stand-off distance for the smallest model. Finally, it was shown that the free-stream conditions were in thermodynamic equilibrium. This was found true for the operating conditions quoted, and for reactant concentrations $0{\cdot}2 < \omega_R < 0{\cdot}4$. The determination of equilibrium states was made by the application of a simplified sudden-freezing analysis (Bray 1959) previously tested for this system (Wegener 1960).

Experimentally, we deal with a non-dimensional stand-off distance function

$$\Delta/R = \Delta/R(M_\infty, \omega_R, \alpha_\infty, D). \tag{9}$$

In (9) the free-stream conditions are denoted by the subscript ∞, with $\omega_R =$ constant throughout. The Mach number is defined by $M_\infty = u_\infty/a_\infty$, where a_∞ is the free-stream, frozen sound speed. The Damköhler parameter, D, is given by (7) or (8). We see from (9) that the stand-off distance depends on four variables, and to study the effect of D on the stand-off distance only, M_∞, ω_R and α_∞ must be held constant. The variation of D, with the other parameters held constant, may be readily accomplished by varying the characteristic flow time of (3) by the use of spheres with different radii, R. We note that the absolute value of ω_R governs the properties of the mixture. In addition, the amount of heat absorbed by the reaction to change the state of the flow from α_s to $\alpha = 0{\cdot}95\alpha_e$ is determined by ω_R for a fixed D Primarily for this reason there is a dependence of Δ/R on ω_R

even for equilibrium flow ($D = \infty$). Practical problems such as this often make a separation of variables difficult. For example, in experiments conducted in firing ranges the Mach number is usually changed in order to induce different degrees of dissociation in the shock layer. Returning to our experiments, it is finally needed to measure Δ for a number of spheres of different R exposed to a fixed free stream.

Typical initial filling conditions for the pressure tube are 300°K, 900 Torr, $\omega_R = 0{\cdot}20$, and $\alpha = 0{\cdot}50$. After diaphragm rupture, the steady-state nozzle

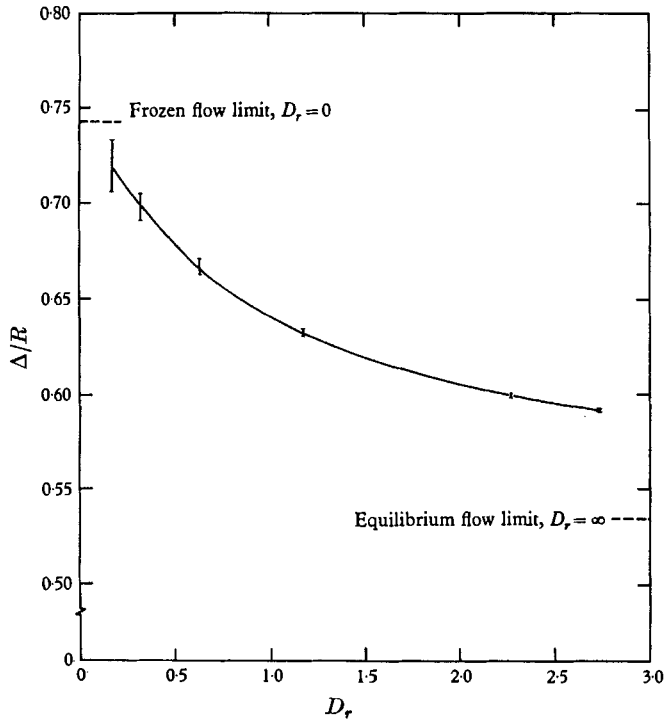

FIGURE 4. Dimensionless shock stand-off distance as a function of the Damköhler parameter, D_r, for $M_\infty = 1{\cdot}37$, $\omega_R = 0{\cdot}216$ and $\alpha_\infty = 0{\cdot}140$.

supply conditions behind the expansion fan are 290°K, 750 Torr, and $\alpha = 0{\cdot}45$. The resulting equilibrium free-stream conditions are $M_\infty = 1{\cdot}4$, $T_\infty = 250$ °K, $p_\infty = 240$ Torr, $\alpha = 0{\cdot}15$, and $\rho_\infty = 5 \times 10^{-4}$ g cm^{-3}. Spheres of different sizes are photographed about 10 ms after the start of steady nozzle flow. Shadowgraphs are obtained in parallel light of about 0·5 μs duration. A Leica camera with a f: 4·5, 135 mm lens using Kodak Tri-X Pan film is focused on a plane removed by 0·2 mm from the centreline of the test section. Only a small portion of the bow shock wave is in focus permitting a well-defined measurement of Δ on photographs such as the one shown in figure 3, plate 1. (The spots seen in this figure result from the presence of small air bubbles in the lens which was used to produce the parallel light.) The narrow white zone surrounding the black image of the sphere is also visible on 'no flow' pictures.

Measurements of the stand-off distance are taken directly from negatives with a travelling microscope at a 60:1 magnification. A reference line shown on the photograph indicates the flow direction. The distance of the centre of the apparent shock wave to the stagnation point is read. For flows with dry nitrogen, typical values of $\Delta/R = 0{\cdot}628$ and $\Delta/R = 0{\cdot}614$ are found for $\frac{1}{32}$ and $\frac{5}{8}$ in. spheres respectively at $M_\infty = 1{\cdot}4$. The scatter in Δ/R found by repeated measurements is about $\pm 2\,\%$ for the smallest sphere and it is about one-tenth of this value for the largest one. The spheres of different radii were mounted in the test section in such a way that their bow shock appeared at the same location. The apparent $2{\cdot}5\,\%$ increase of the mean values of Δ/R from the largest to the smallest sphere is primarily caused by the slightly non-uniform flow in the wedge-type nozzle with a Mach number gradient of about $\Delta M/\Delta x = 1{\cdot}5 \times 10^{-2}$ cm^{-1} at the model location.

Typical results such as those shown in figure 4 for fixed free-stream conditions may be found as discussed. The error bars indicate the experimental uncertainties. The greatest error stems from the reading of the stand-off distance. Therefore the results for the small spheres at the low values of the Damköhler parameter show the longest error bars. On figure 4 we also show estimated values of $D_r = 0$ and $D_r = \infty$. These bounds were obtained from an empirical correlation of $\Delta/R(\rho_s/\rho_\infty)$ for flow about spheres in perfect gases given by Ambrosio & Wortman (1962). In such a form, the stand-off distance is not strongly dependent on the physical properties of the gas. After computing the density ratio for frozen and equilibrium flow across normal shocks, the corresponding stand-off distance values were obtained from the cited empirical formula.

4. Results and discussion

Since Δ/R for blunt bodies is highly sensitive to Mach number changes at low supersonic speeds we first compare our results obtained with dry nitrogen with others found in the literature. Figure 1 reveals a surprising scatter of the data of various experiments. This state of affairs is at least partially due to the many different experimental techniques employed. Our results fit well and they seem to be little affected by the slight Mach number gradient in the nozzle. Qualitatively, the non-equilibrium process can be seen directly in figure 3, plate 1, by observing the relative shading of the photograph in the shock layer. The nitrogen dioxide (NO_2) is brown and absorbs in the visible light region while N_2O_4 and N_2 are clear. Although there is a density increase of NO_2 and consequently a concentration increase across the weak (low Mach number) frozen shock, the pronounced darkening visible in figure 3 occurs only some distance downstream from the shock. This distance corresponds to a relaxation length, related to $\tau_r u_s$ or $\tau_\phi u_s$, past which the dissociation of N_2O_4 becomes noticeable in a marked increase of the NO_2 concentration. The recombination reaction, $2NO_2 \rightarrow N_2O_4$, sets in farther down in the expansion regions about the sphere and this effect leads to a return of the lighter shade. Also seen in the photograph is the out-of-focus interaction of the bow shock wave and the boundary layers on the sidewall.

The final result of this work is presented in figure 5. The error bars of figure 4 have been omitted and each point represents a direct Δ/R measurement in an environment whose properties were determined as shown before. The trend of the results between the two limits is found to be as expected by Freeman (1958). This is not surprising because our gas mixture lends itself to a description in terms of Lighthill's ideal dissociating gas (Lighthill 1957) as adapted to non-

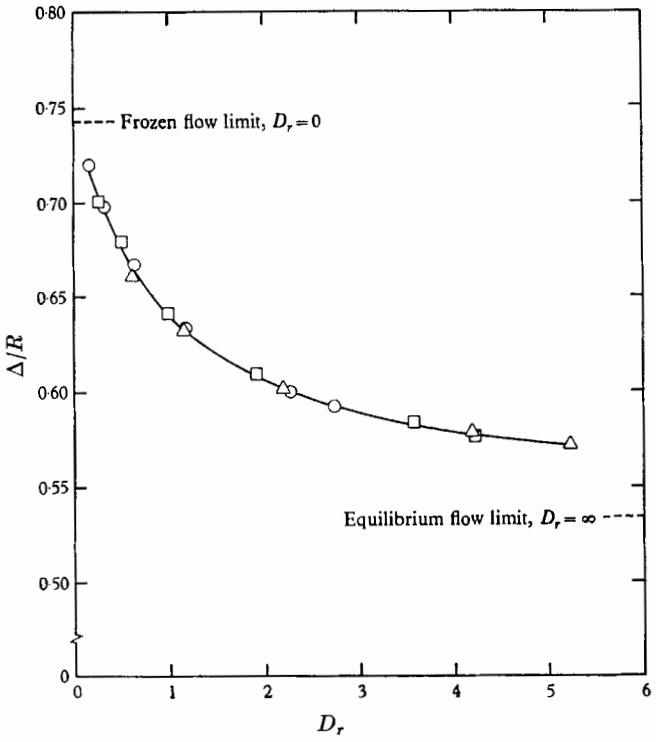

FIGURE 5. Dimensionless shock stand-off distance as a function of the Damköhler parameter, D_r, for: ○, $M_\infty = 1{\cdot}37$, $\omega_R = 0{\cdot}216$, $\alpha_\infty = 0{\cdot}140$; □, $M_\infty = 1{\cdot}36$, $\omega_R = 0{\cdot}301$, $\alpha_\infty = 0{\cdot}151$; △, $M_\infty = 1{\cdot}36$, $\omega_R = 0{\cdot}400$, $\alpha_\infty = 0{\cdot}178$.

equilibrium flow by Freeman. We observe a rapid drop of Δ/R at low values of D_r followed by a more gradual approach to the limiting value at $D_r = \infty$. We note that changes of ω_R by about a factor of two do not lead to substantially different dimensionless stand-off distance values. Much of the effect of the higher reactant concentration is, of course, already implicit in the calculation of D_r. The results shown in figure 5 are similar to those calculated for the non-equilibrium parameter D_ϕ given by (3), (6) and (8). For fixed Δ/R we simply find $D_\phi = 5D_r$.

The results shown in figure 5 may be compared more directly with the available theoretical work by the introduction of a normalized stand-off distance parameter.† We can write

$$\delta = \frac{\Delta - \Delta_e}{\Delta_f - \Delta_e}, \tag{10}$$

† The comparison that follows was suggested to the authors by a reviewer of this paper. We are most grateful for this proposal.

where the subscripts e and f again denote the equilibrium and frozen stand-off distance values respectively. Next we compute $\delta(D_r)$ for the experiments shown in figure 5. A similar calculation may be made for the theoretical results of Freeman (1958) and Conti (1966). For fixed values of δ, we can then plot the different non-equilibrium parameters with respect to each other. It is found that the results lie approximately on straight lines, suggesting that a fixed factor relates the widely different relaxation parameters to each other. This procedure avoids the cumbersome direct calculation of our results in terms of the relaxation parameters used by different authors. The solid curve shown in figure 5 closely represents the theoretical work cited and related to our experiments by the above procedure. There is some scatter at the lowest values of $D_r < 1$ where our results are least reliable.

Finally, the results in figure 5 are in reasonable agreement with a similar function proposed for vibrational relaxation (Blythe 1963) by Hayes & Probstein (1966, p. 385). This procedure finally lends itself to reversal in order to find the relaxation time of a single non-equilibrium mode from the variation of the measured stand-off distance. However, owing to the sensitivity of results obtained with (10) to the exact knowledge of the bounding Δ/R-values, care needs to be exercised in the application of the comparison.

Discussions with our colleague Dr Boa-Teh Chu are gratefully acknowledged. The work described was sponsored by the Arnold Engineering Development Center, Air Force Systems command, U.S.A.F.

REFERENCES

Ambrosio, A. & Wortman, A. 1962 Stagnation-point shock-detachment distance for flow around spheres and cylinders in air. *J. Aerospace Sci.* **29**, 875.

Becker, E. 1958 Reibungswirkungen beim Rohrwindkanal. *Mitteilungen aus dem Max Planck Institut für Strömungsforschung und der Aerodynamischen Versuchsanstalt*, no. 20.

Blythe, P. A. 1963 The effects of vibrational relaxation on hypersonic flow past blunt bodies. *Aeronaut. Quart.* **14**, 357.

Bray, K. N. C. 1959 Atomic recombination in a hypersonic wind tunnel nozzle. *J. Fluid Mech.* **6**, 1.

Carrington, R. & Davidson, N. 1953 Shock waves in chemical kinetics: the rate of dissociation of N_2O_4. *J. Phys. Chem.* **57**, 418.

Conti, R. J. 1966 A theoretical study of non-equilibrium blunt-body flows. *J. Fluid Mech.* **24**, 65.

Damköhler, G. 1936 Einflusse der Strömung, Diffusion und des Wärmeüberganges auf die Leistung von Reaktionsöfen. I. Allgemeine Gesichtspunkte für die Übertragung eines chemischen Prozesses aus dem Kleinen ins Grosse. *Z. Elektrochem.* **42**, 846.

Eckerman, J. 1961 The measurement of the rate of dissociation of oxygen at high temperatures. Ph.D. Thesis, Catholic University of America, Washington, D.C.

Förster, T. & Geib, K. H. 1934 Die theoretische Behandlung chemischer Reaktionen in strömenden Systemen. *Ann. Phys.* **20**, 250.

Freeman, N. C. 1958 Non-equilibrium flow of an ideal dissociating gas. *J. Fluid Mech.* **4**, 407.

Hall, J. G., Eschenroeder, A. Q. & Marrone, P. V. 1962 Blunt-nose inviscid airflows with coupled non-equilibrium processes. *J. Aerospace Sci.* **29**, 1038.

HALL, J. G. & TREANOR, G. E. 1968 Nonequilibrium effects in supersonic-nozzle flows. *Cornell Aeronautical Laboratory Rep.* no. CAL-163.

HAYES, W. D. & PROBSTEIN, R. F. 1966 *Hypersonic Flow Theory*, Vol. I. New York: Academic Press.

HEBERLE, J. W., WOOD, G. P. & GOODERUM, P. B. 1950 Data on shape and location of detached shock waves on cones and spheres. *NACA* TN 2000.

JENKINS, A. H., JENKINS, B. Z. & JOHNSON, L. H. 1966 Transonic and low supersonic shock shape solutions. *AIAA J.* **4**, 1483.

KENDALL, J. M. 1959 Experiments on supersonic blunt-body flows. *Rep. Jet Propulsion Lab.* no. 20-372. California Institute of Technology, Pasadena.

LICK, W. 1960 Inviscid flow of a reacting mixture of gases around a blunt body. *J. Fluid Mech.* **7**, 128.

LIGHTHILL, M. J. 1957 Dynamics of a dissociating gas. Part 1. Equilibrium flow. *J. Fluid Mech.* **2**, 1.

LOBB, K. R. 1963 Experimental measurement of shock detachment distance on spheres fired in air at hypervelocities. *High Temperature Aspects of Hypersonic Flow.* New York: Pergamon Press.

LUDWIEG, H. 1955 Der Rohrwindkanal. *Z. Flugwiss.* **3**, 206.

LUDWIEG, H. 1957 The tube wind tunnel, a special type of blowdown tunnel. *AGARD Rep.* no. **143**.

LUN'KIN, YU. P. & POPOV, F. D. 1966 Vibration-dissociation relaxation on supersonic flow around blunt bodies. *Soviet Phys. Tech. Phys.* **11**, 491.

MOECKEL, W. E. 1949 Approximate method for predicting form and location of detached shock waves ahead of plane or axially symmetric bodies. *NACA* TN 1921.

NAGAMATSU, H. T. 1949 Theoretical investigation of detached shock. Ph.D. Thesis, California Institute of Technology, Pasadena.

SCHLICHTING, H. 1960 *Boundary Layer Theory.* New York: McGraw-Hill.

SCHWARTZ, R. N. & ECKERMAN, J. 1956 Shock location in front of a sphere as a measure of real gas effects. *J. Appl. Phys.* **27**, 169.

VAN DYKE, M. D. 1958 The supersonic blunt-body problem—review and extension. *J. aeronaut. Sci.* **25**, 485.

VAN DYKE, M. D. & GORDON, H. D. 1959 Supersonic flow past a family of blunt axisymmetric bodies. *NASA* TR R-1.

WEGENER, P. P. 1958 Measurement of rate constants of fast reactions in a supersonic nozzle. *J. Chem. Phys.* **28**, 724.

WEGENER, P. P. 1960 Experiments on the departure from chemical equilibrium in a supersonic flow. *ARS Jl.* **30**, 322.

WEGENER, P. P., CHU, B-T. & KLIKOFF, W. A. 1965 Weak waves in relaxing flows. *J. Fluid Mech.* **23**, 787.

ZELDOVICH, YA. B. & RAISER, YU. P. 1966 *Physics of Shock Waves and High-Temperature Hydrodynamic Phenomena*, Vol. I. New York: Academic Press.

ZIENKIEWICZ, H. K. & MALLOCH, I. D. 1968 Establishment of the bow-wave in the supersonic flow of carbon dioxide past a sphere. *Aeronaut. Quart.* **19**, 51.

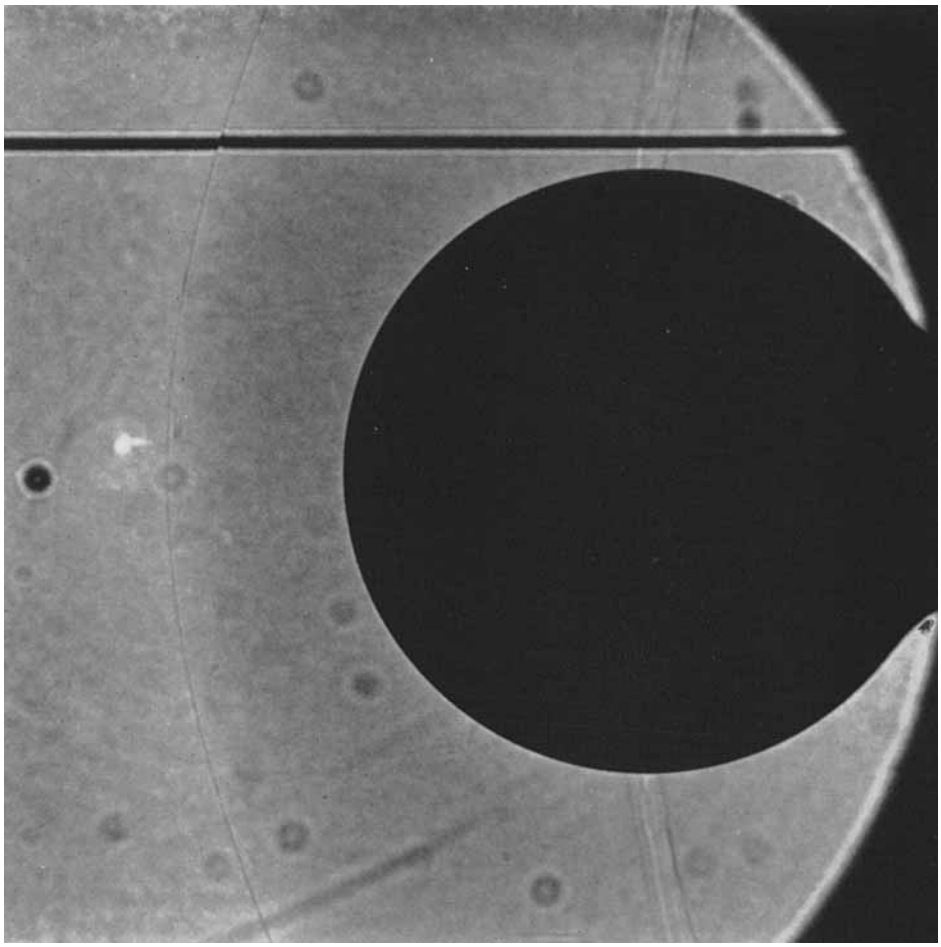

FIGURE 3. Sharp-focus shadowgraph of the non-equilibrium flow field about a $\frac{1}{2}$ in. diameter sphere at $M_\infty = 1{\cdot}36$, $\omega_R = 0{\cdot}3$ and $\alpha_\infty = 0{\cdot}15$. Flow from left to right.